J Bionic Eng 15 (2018) 907–913
DOI: https://doi.org/10.1007/s42235-018-0077-x

Journal of Bionic Engineering
http://www.springer.com/journal/42235

Fabrication of Porous Mg-Zn Scaffold through Modified Replica Method for Bone Tissue Engineering

Amir Hamed Aghajanian[1], Bijan Abbasi Khazaei[1*], Mohammad Khodaei[2], Mohammad Rafienia[3]

1. *Department of Materials Engineering*, *Faculty of Engineering*, *Razi University*, *Kermanshah*, *Iran*
2. *Dental Research Center*, *School of Dentistry*, *Isfahan University of Medical Sciences*, *Isfahan* 81746-73461, *Iran*
3. *Biosensor Research Center*, *Isfahan University of Medical Sciences*, *Isfahan* 81744176, *Iran*

Abstract

Biodegradable scaffolds are essential parts in hard tissue engineering. A highly porous magnesium-zinc (Mg-Zn 4 wt.%) scaffold with different Mg-Zn powder to liquid media ratios (50 wt.%, 70 wt.% and 90 wt.%) and different concentrations of ethanol (0 vol.%, 10 vol.%, 20 vol.% and 40 vol.%) were prepared through modified replica method. The mechanical properties were assessed through compression test and the structures of scaffolds were examined by Scanning Electron Microscope (SEM). Results show that, the increase in Mg-Zn powder to liquid media ratio (50 wt.% to 90 wt.%) in ethanol free slurry, increases the thickness of struts (37 μm to 74 μm) and the plateau stress (0.5 MPa to 1.4 MPa). The results obtained from X-ray Diffractometry (XRD) and compression test indicate that consuming ethanol in liquid media of replica, results in higher plateau stress by 46% due to less Mg-water reaction and no formation of $Mg(OH)_2$ in the scaffold. The results of porosity measurement indicate that water-ethanol mixture composition and different solid fractions have no significant effects on true and apparent porosities of the fabricated scaffolds.

Keywords: porous magnesium scaffold, replica method, Mg-Zn powder to water ratio, mechanical properties

1 Introduction

Biodegradable scaffolds are a class of implants that degrade gradually in human body with a suitable host reaction elicited by the released degradation products. They should disappear entirely upon fulfilling the mission of supporting the restoration of bone defects leaving no implant residues. Therefore, no further surgical operation is required for the implant removal[1,2].

It has been shown in the literature that the architecture of a porous implant has a great effect on the bone ingrowth into the pore space[3]. Porous structure provides adequate space for cell migration, adhesion, proliferation and differentiation, allowing new bone tissue ingrowth[4]. Although porosity is necessary for scaffolds, however, it considerably reduces the scaffold's strength[1]. Recently, porous Mg and Mg alloys have been specially suggested as metallic scaffolds[5–7], because of mechanical properties close to those of human bone, *in vivo* biodegradation characteristics in body fluids and also natural ionic content that may have important functional roles in physiological systems[1].

A variety of processing methods have been developed to fabricate porous Mg based scaffolds, such as powder metallurgy[6,8,9], laser perforation[10,11], titanium wire space holder[12], hydrogen injection[13] and negative salt pattern molding[14]. In addition, there are some methods like freeze-casting[15], plasma-spray[16], 3D rapid prototyping[17] and Polymeric Sponge Replication (PSR) method[18–22], which have been used to fabricate some metallic/ceramic based scaffolds. The PSR method has received particular attention because it can provide very high porosity with good interconnections between pores[23]. In this method, ceramic/metallic powders are mixed with a solver, dispersant and binder into slurry, which will be used to impregnate a polymer foam template. After drying, the dispersant, binder and polymer foam are removed and the powder framework is sintered. The metallic/ceramic foam will replicate the polymer foam structure. Therefore, it is possible to fabricate highly porous open-cell metallic/ceramic foam with a uniform cell structure similar to the polymer foam[20,22,24]. The PSR method has been used to fabricate hydroxyapatite[19,20] and titanium[21,22,24] based

***Corresponding author:** Bijan Abbasi Khazaei
E-mail: biabkh1969@gmail.com

Table 1 Coding, condition, thickness of the struts and plateau stress of different samples

Name of the sample	Mg-Zn powder (wt.%)	Ethanol in liquid media (vol.%)	Mean thickness of the struts (μm)	Plateau stress (MPa)
MZ50-E0	50	0	37 ± 7	0.50 ± 0.05
MZ70-E0	70	0	58 ± 8	0.75 ± 0.06
MZ90-E0	90	0	74 ± 7	1.40 ± 0.08
MZ70-E10	70	10	57 ± 9	0.86 ± 0.05
MZ70-E20	70	20	56 ± 8	0.98 ± 0.06
MZ70-E40	70	40	58 ± 8	1.10 ± 0.07

scaffolds. Lee *et al*.[21] produced a titanium based scaffold using PSR method with porosity about 70% and compressive strength of 18 MPa. They prepared their slurry by dispersing TiH_2 powder in ethanol containing of triethyl phosphate as a dispersant and polyvinylbutyl as a binder. Using the same method, Ahmad *et al*.[24] fabricated titanium scaffolds with porosity up to 80% and compressive strength of 14.85 MPa. Wang *et al*.[25] have introduced a mixture of deionized water and ethanol as a modified solvent to the preparation of titanium slurry in PSR method. The addition of ethanol to the titanium slurry improved compressive strength of titanium scaffold by increasing the compactness of the skeleton.

It seems that, the modified PSR method has not been applied for the fabrication of the magnesium-zinc scaffold so far. Hence, the main objective of this research is to assess the processability of highly porous magnesium-zinc (Mg-Zn 4 wt.%) scaffold through modified PSR method. The effect of processing variables such as the compositions of water-ethanol mixture and the powder metal to liquid media ratios on microstructure and mechanical strength of the scaffolds has been studied.

2 Materials and methods

2.1 Porous Mg-Zn scaffold fabrication process

Polyurethane (PU) sponges (MEAY Co., Ltd. China; average pore size of 300 μm – 700 μm) as the sacrificial template of 10 × 10 × 10 mm dimension were dipped into Mg-Zn 4 wt.% slurry with 50 wt.%, 70 wt.% and 90 wt.% of Mg-Zn powder (Mg: particle size of 63 μm, Merck, CAS No. 7439-95-4; Zn: particle size of 10 μm, Merck, CAS No. 7440-66-6, Germany), 1.5 wt.% of polyvinyl alcohol (PVA) and 1 wt.% of Dolapix in water-base liquid media (distilled water with 0 vol.%, 10 vol.%, 20 vol.% and 40 vol.% ethanol). Excess slurry was removed from the PU templates by squeezing the sponge to avoid PU template pore filling. All struts of the PU sponge should be covered with magnesium slurry. The obtained green magnesium foam was dried for 24 h at room temperature; then, it was exposed to 10^{-5} mbar vacuum and heated at 450 ˚C for 1 h for polyurethane removal. An increase in temperature from 450 ˚C to 550 ˚C, for 2 h allows magnesium sintering. The process was carried out at heating and cooling rate of 5 ˚C·min^{-1}. Different coding and condition for the samples are shown in Table 1.

2.2 Microstructural observation

The effect of Mg-Zn powder to liquid media ratio on microstructure of scaffolds was characterized through Scanning Electron Microscope (SEM; XL 30, Philips, Netherlands). The samples were gold coated through a sputter coater before observation.

2.3 Porosity measurement

The amount of porosity was measured according to ASTM B962 standard by Archimedes method with distilled water impregnation. The apparent (interconnected) porosity was obtained as:

$$\text{Apparent porosity} = \frac{W_w - W_d}{W_w - W_s} \times 100, \quad (1)$$

where W_d, W_w and W_s are the weight of the sample, in air, including water and suspended in water, respectively.

The true porosity including both closed and apparent porosities could be calculated according to the following equation:

$$\text{Ture porosity} = 1 - \frac{W_d}{\rho(W_w - W_s)} \times 100, \quad (2)$$

where ρ is the theoretical density of Mg-Zn 4 wt.%. The

measurement was performed for three times in order to obtain the mean value of true and apparent porosities.

2.4 Phase identification

To assess the probable phases formed during this process (initial powders, fabricated template in water, fabricated template in ethanol-water mixture and sintered sample), X-ray diffraction (XRD: Philips, X'Pert-MPD, Netherland) was applied as the radiation source Cu-Kα (λ = 1.5405 A˚), at 40 kV, at the rate of $2\theta = 1^{\circ}\cdot\text{min}^{-1}$ in the range of $2\theta = 20^{\circ} - 80^{\circ}$.

2.5 Compression test

Compression test for the fabricated cubic porous samples of (10×10×10 mm) was carried out through an universal testing machine (INSTRON 5566S, USA), according to ISO 13314:2011 at a 1 mm·min^{-1} cross-speed. The test was run on the samples (with the same condition) for three times in order to estimate the mean value and standard deviation of the plateau stress of the sintered samples.

3 Results and discussion

3.1 SEM observation

The morphology and microstructure of raw materials is shown in Fig. 1. It is evident that, polyurethane sponge contains of interconnected pores smaller than 700 μm (Fig. 1a) and the particles shape of magnesium and zinc powders are irregular (Fig. 1b) and spherical (Fig. 1c), respectively. The microstructure of the sintered samples at different magnifications is shown in Fig. 2, in which, the thickness of Mg-Zn scaffolds struts is increased by an increase in Mg-Zn powder to liquid media ratio (Figs. 2a – 2c).

Microstructure of the scaffolds fabricated by consuming different compositions of water-ethanol mixtures, indicate that, no differences is observed among different samples. According to the results obtained through SEM

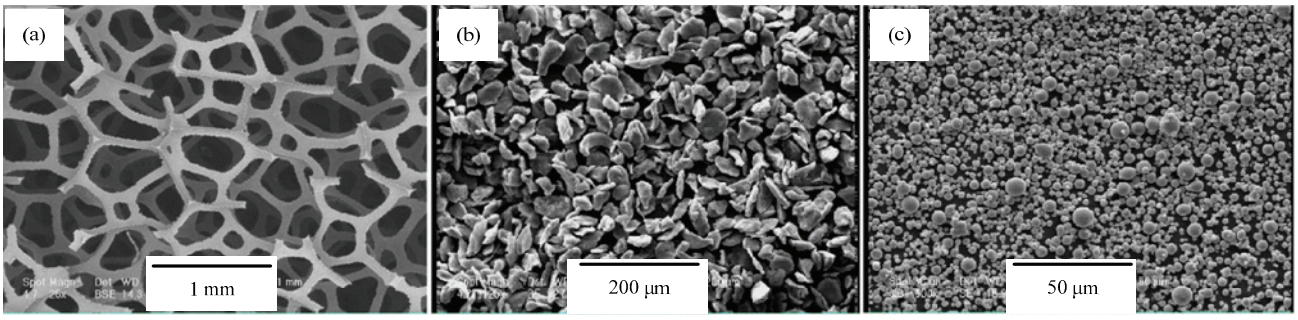

Fig. 1 SEM micrographs of raw materials. (a) Polyurethane sponge; (b) particles of magnesium powder; (c) particles of zinc powder.

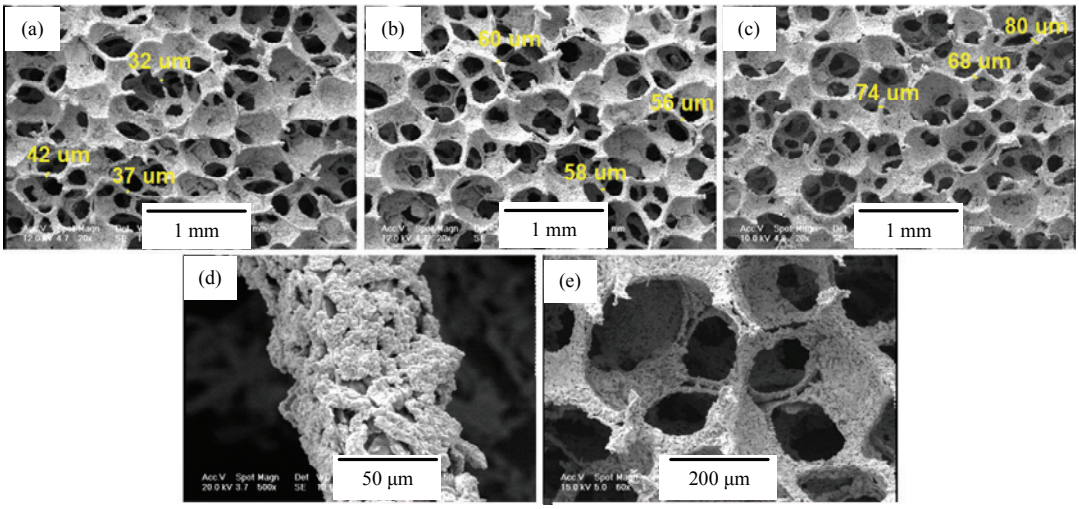

Fig. 2 SEM micrographs for different Mg-Zn porous scaffold fabricated by Mg-Zn powder to liquid media ratio of (a) 50 wt.%, (b) 70 wt.%, (c) 90 wt.% after sintering, (d) a strut of scaffold at higher magnification and (e) hollow struts (polyurethane removal).

observations, almost all pores of the scaffold are interconnected, the magnesium particles are completely welded to each other (Fig. 2d), polyurethane is completely removed from the core (center) of struts, and hollow magnesium based struts are formed (Fig. 2e).

According to the results obtained through ImageJ processing of the SEM images, the struts thickness of the Mg-Zn scaffolds increases from 37 μm to 74 μm, by an increase in the metal powder content of the slurry from 50 wt.% to 90 wt.%. It is evident that the ethanol content of the liquid media had no effect on the thickness of the struts.

3.2 Phase identification

Results of XRD are exhibited in Fig. 3, indicating that initial powders (mixture of Mg-Zn powders) consist of merely pure magnesium and zinc phases. The dried template fabricated in water (MZ70-E0) before sintering, was crushed and analyzed. As seen in the figure, in this sample, $Mg(OH)_2$ is formed, indicating the interaction between magnesium and water during template fabrication process; while $Mg(OH)_2$ is not formed in the fabricated template where water-ethanol mixture (MZ70-E40) is consumed. It is assumed that, ethanol inhibits the reaction between water and magnesium during template fabrication process. Although $Mg(OH)_2$ is not observed in the sintered samples, but small peak of MgO is observed for both fabricated templates. Direct oxidation of magnesium or decomposition of $Mg(OH)_2$ may result in MgO formation. It is suggested that, during sintering, the small amount of MgO phase reduces the strength of bonding between particles. Therefore, it is expected that, the compressive strength of samples fabricated in water-ethanol slurry could be higher due to less Mg-water reaction.

The XRD pattern of the sintered sample consists of sharp peaks of pure magnesium phase and small peaks of MgO phase. No intermetallic phase is observed between magnesium and zinc in the pattern because of their low concentration, which corresponds to the findings of Seyedraoufi *et al*.[5].

3.3 Porosity of samples

The results of porosity measurement indicate that composition of water-ethanol mixture has no significant

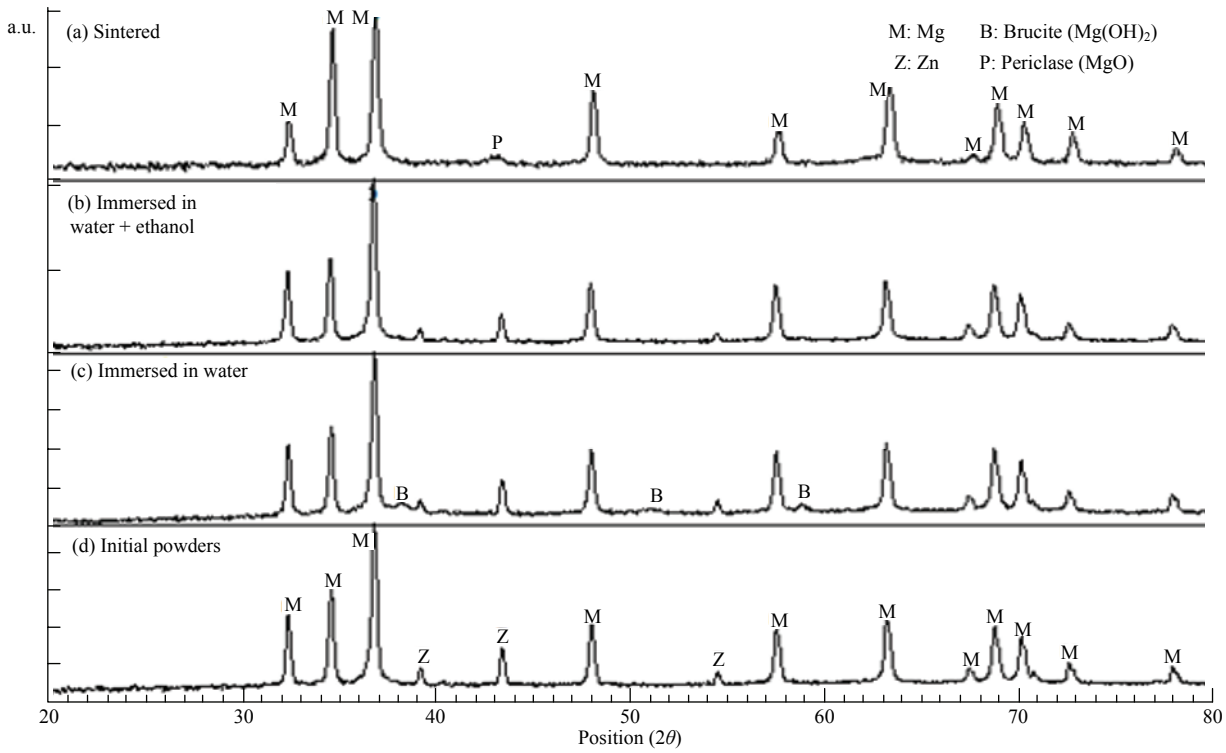

Fig. 3 X-ray diffraction pattern of (a) sintered Mg-Zn scaffold, (b) immersed template in water + ethanol (MZ70-E40) before sintering, (c) immersed template in water (MZ70-E0) before sintering, and (d) mixture of initial Mg-Zn powders.

effect on true and apparent porosities of magnesium scaffolds. In (MZ50-E0), (MZ70-E0) and (MZ90-E0) samples, with an increase in the solid fraction, true porosity is decreased from 82% to 81% and the apparent porosity is decreased from 81% to 79%. Decreasing of the porosities can be attributed to the thickening of the struts which would results in the higher compressive strength as shown in next section.

Porosity measurement shows that, for all cases, the open porosity ratio is in excess of 0.98, indicating that most cells are interconnected. It should be mentioned that, cancellous bones consist of an interconnected porous structure with the porosity of 30% to 95%[1], and the interconnectivity of pores and appropriate porosity are necessary conditions for successful cell viability in 3D scaffolds[26]. Therefore, the fabricated magnesium based scaffold could be intentioned from two aspects of interconnectivity and the amount of porosity.

Comparing the results of porosity measurement, indicates that water-ethanol mixture composition and different solid fractions have no significant effects on true and apparent porosities of the fabricated scaffolds.

3.4 Compressive strength

The compressive engineering stress–strain curves of different samples are illustrated in Fig. 4. Different coding, condition, mean thickness of the struts and plateau stress for different sintered samples are shown in Table 1.

According to the results obtained from the compression tests, the plateau stress of the sintered scaffolds increases from 0.5 MPa to 1.4 MPa, as the solid content of Mg-Zn powder in ethanol free slurry increases from 50 wt.% to 90 wt.%. This phenomenon is due to the thickening of the struts (Fig. 2). It is evident that by increasing the solid content of Mg-Zn powder in ethanol free slurry from 50 wt.% to 90 wt.%, the thickness of the struts of scaffold increases from 37 μm to 74 μm, where higher force is required to compress the pores of the scaffold.

As shown in Fig. 4 and Table 1, the plateau stresses of MZ70-E0, MZ70E-10, MZ70-E20 and MZ70-E40, are about 0.75 MPa, 0.86 MPa, 0.98 MPa and 1.1 MPa, respectively. It is evident that the plateau stress of

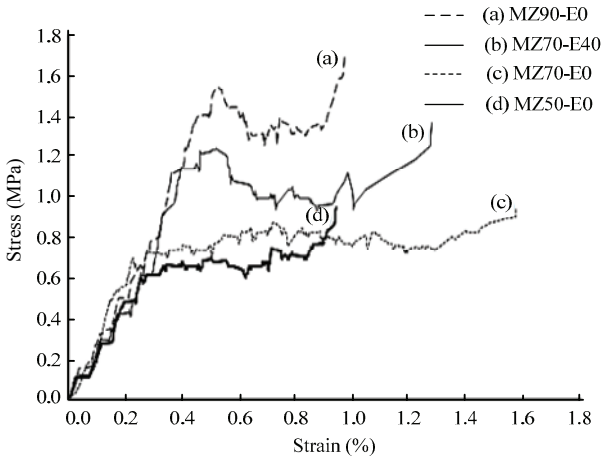

Fig. 4 The engineering stress-strain curve for different Mg-Zn porous samples.

Mg-Zn scaffold fabricated through modified replica method increases with the ethanol content of slurry, because the ethanol inhibits the Brucite/MgO formation on the surface of magnesium powder beads, allowing their better diffusion. Although, the compressive strength level of the samples is relatively low, but it is in cancellous bone strength range (0.2 MPa – 80 MPa[1]).

In general, the authors here recommend consuming water-ethanol mixture for Mg-Zn scaffold fabrication in which replica method is adopted. This mixture inhibits Brucite/MgO formation of Mg powder in the slurry, thus, higher compressive strength could be obtained.

4 Conclusion

Highly porous Mg-Zn 4 wt.% scaffolds were fabricated through modified replica method. Different concentrations of ethanol with different metal powder to liquid media ratios were consumed and applied for scaffold fabrication. The struts thickness and the plateau stress increase with the Mg-Zn powder to liquid media ratio. Water-ethanol mixture composition and different solid fractions have no considerable effects on true and apparent porosities of the fabricated scaffolds. Consuming ethanol in the slurry inhibits the $MgO/Mg(OH)_2$ formation on the surface of magnesium powder beads which results in higher plateau stress of the scaffolds by 46%. The compressive strength of fabricated porous scaffolds made of reactive metals through replica method is subject to the struts thickness and its bonding strength.

Acknowledgment

The authors gratefully acknowledge support from Isfahan University of Medical Sciences.

References

[1] Yazdimamaghani M, Razavi M, Vashaee D, Moharamzadeh K, Boccaccini A R, Tayebi L. Porous magnesium-based scaffolds for tissue engineering. *Materials Science and Engineering*: *C*, 2017, **71**, 1253–1266.

[2] Senatov F, Anisimova N, Kiselevskiy M, Kopylov A, Tcherdyntsev V, Maksimkin A. Polyhydroxybutyrate/hydroxyapatite highly porous scaffold for small bone defects replacement in the nonload-bearing parts. *Journal of Bionic Engineering*, 2017, **14**, 648–658.

[3] Li J P, Li S H, Van Blitterswijk C A, De Groot K. A novel porous Ti6Al4V: Characterization and cell attachment. *Journal of Biomedical Materials Research Part A*, 2005, **73**, 223–233.

[4] Ghomi H, Emadi R, Javanmard S H. Fabrication and characterization of nanostructure diopside scaffolds using the space holder method: Effect of different space holders and compaction pressures. *Materials & Design*, 2016, **91**, 193–200.

[5] Seyedraoufi Z S, Mirdamadi S. Synthesis, microstructure and mechanical properties of porous Mg-Zn scaffolds. *Journal of the Mechanical Behavior of Biomedical Materials*, 2013, **21**, 1–8.

[6] Yazdimamaghani M, Razavi M, Vashaee D, Tayebi L. Microstructural and mechanical study of PCL coated Mg scaffolds. *Surface Engineering*, 2014, **30**, 920–926.

[7] Yazdimamaghani M, Razavi M, Vashaee D, Pothineni V R, Assefa S, Köhler G A, Rajadas J, Tayebi L. *In vitro* analysis of Mg scaffolds coated with polymer/hydrogel/ceramic composite layers. *Surface and Coatings Technology*, 2016, **301**, 126–132.

[8] Zhuang H Y, Han Y, Feng A L. Preparation, mechanical properties and *in vitro* biodegradation of porous magnesium scaffolds. *Materials Science and Engineering*: *C*, 2008, **28**, 1462–1466.

[9] Yazdimamaghani M, Razavi M, Vashaee D, Tayebi L. Surface modification of biodegradable porous Mg bone scaffold using polycaprolactone/bioactive glass composite. *Materials Science and Engineering*: *C*, 2015, **49**, 436–444.

[10] Geng F, Tan L L, Zhang B C, Wu C F, He Y L, Yang J Y, Yang K. Study on beta-TCP coated porous Mg as a bone tissue engineering scaffold material. *Journal of Materials Science & Technology*, 2009, **25**, 123–129.

[11] Chen Z T, Mao X L, Tan L L, Friis T, Wu C T, Crawford R, Xiao Y. Osteoimmunomodulatory properties of magnesium scaffolds coated with β-tricalcium phosphate. *Biomaterials*, 2014, **35**, 8553–8565.

[12] Jiang G F, He G. A new approach to the fabrication of porous magnesium with well-controlled 3D pore structure for orthopedic applications. *Materials Science and Engineering*: *C*, 2014, **43**, 317–320.

[13] Gu X N, Zhou W R, Zheng Y F, Liu Y, Li Y X. Degradation and cytotoxicity of lotus-type porous pure magnesium as potential tissue engineering scaffold material. *Materials Letters*, 2010, **64**, 1871–1874.

[14] Witte F, Ulrich H, Rudert M, Willbold E. Biodegradable magnesium scaffolds: Part 1: Appropriate inflammatory response. *Journal of Biomedical Materials Research Part A*, 2007, **81**, 748–756.

[15] Li J C, Dunand D C. Mechanical properties of directionally freeze-cast titanium foams. *Acta Materialia*, 2011, **59**, 146–158.

[16] Takemoto M, Fujibayashi S, Neo M, Suzuki J, Kokubo T, Nakamura T. Mechanical properties and osteoconductivity of porous bioactive titanium. *Biomaterials*, 2005, **26**, 6014–6023.

[17] Ryan G E, Pandit A S, Apatsidis D P. Porous titanium scaffolds fabricated using a rapid prototyping and powder metallurgy technique. *Biomaterials*, 2008, **29**, 3625–3635.

[18] Chen Q Z, Thompson I D, Boccaccini A R. 45S5 bioglass®-derived glass–ceramic scaffolds for bone tissue engineering. *Biomaterials*, 2006, **27**, 2414–2425.

[19] Teixeira S, Rodriguez M A, Pena P, De Aza A H, De Aza S, Ferraz M P, Monteiro F J. Physical characterization of hydroxyapatite porous scaffolds for tissue engineering. *Materials Science and Engineering*: *C*, 2009, **29**, 1510–1514.

[20] Sopyan I, Kaur J. Preparation and characterization of porous hydroxyapatite through polymeric sponge method. *Ceramics International*, 2009, **35**, 3161–3168.

[21] Lee J H, Kim H E, Koh Y H. Highly porous titanium (Ti) scaffolds with bioactive microporous hydroxyapatite/TiO_2 hybrid coating layer. *Materials Letters*, 2009, **63**, 1995–1998.

[22] Manonukul A, Tange M, Srikudvien P, Denmud N, Wattanapornphan P. Rheological properties of commercially pure titanium slurry for metallic foam production using replica impregnation method. *Powder Technology*, 2014, **266**, 129–134.

[23] Jo I H, Shin K H, Soon Y M, Koh Y H, Lee J H, Kim H E. Highly porous hydroxyapatite scaffolds with elongated pores using stretched polymeric sponges as novel template. *Materials Letters*, 2009, **63**, 1702–1704.

[24] Ahmad S, Muhamad N, Muchtar A, Sahari J, Ibrahim M H I, Jamaludin K R, Nor N H M. Development and characterization of titanium alloy foams. *International Journal of Mechanical and Materials Engineering*, 2010, **5**, 244–250.

[25] Wang C L, Chen H J, Zhu X D, Xiao Z W, Zhang K, Zhang X D. An improved polymeric sponge replication method for biomedical porous titanium scaffolds. *Materials Science and Engineering*: *C*, 2017, **70**, 1192–1199.

[26] Sohn D G, Hong M W, Kim Y Y, Cho Y S. Fabrication of dual-pore scaffolds using a combination of wire-networked molding (WNM) and non-solvent induced phase separation (NIPS) techniques. *Journal of Bionic Engineering*, 2015, **12**, 565–574.